Geophysical Journal International

Geophys. J. Int. (2011) **186,** 6–10 doi: 10.1111/j.1365-246X.2011.05052.x

EXPRESS LETTER

Incorporating metamorphism in geodynamic models: the mass conservation problem

György Hetényi,[1] Vincent Godard,[2] Rodolphe Cattin[3] and James A.D. Connolly[1]

[1] *ETH Zürich, Department of Earth Sciences, Clausiusstrasse 25, 8092 Zürich, Switzerland. E-mail: gyorgy.hetenyi@erdw.ethz.ch*
[2] *CEREGE, Europôle Méditerranéen de l'Arbois, BP80, 13545 Aix-en-Provence Cedex 04, France*
[3] *Géosciences Montpellier, Université Montpellier 2, CC60, Pl. E. Bataillon, 34095 Montpellier Cedex 5, France*

Accepted 2011 April 21. Received 2011 April 21; in original form 2011 March 3

SUMMARY

Geodynamic models incorporating metamorphic phase transformations almost invariably assume the validity of the Boussinesq approximation that violates conservation of mass. In such models metamorphic density changes take place without volumetric effects. We assess the impact of the Boussinesq approximation by comparing models of orogeny accompanied by lower crustal eclogitization both with and without the approximation. Our results demonstrate that the approximation may cause errors approaching 100 per cent in characteristic measures of orogenic shape. Mass conservation errors in Boussinesq models amplify with model time. Mass conservative models of metamorphism are therefore essential to understand long-term tectonic evolution and to assess the importance of the different geodynamic processes.

Key words: Ultra-high pressure metamorphism; Phase transitions; Continental tectonics: compressional; Tectonics and landscape evolution; Dynamics of lithosphere and mantle; Mechanics, theory, and modelling.

1 INTRODUCTION

Geodynamic models of the solid Earth simulate deformation (i.e. collision in the lithosphere and convection in the mantle). They may account for a number of processes that act as the driving forces for deformation, such as convergence and metamorphic phase changes. The models generally solve three constitutive conservation equations: the momentum conservation law, the heat equation and the continuity in mass of the system (e.g. Cserepes *et al*. 1988). Each of these equations can be simplified according to the specific features of the investigated physical problem. In this study we focus on mass conservation, as its simplifications are the most relevant in affecting deformation and in accounting for metamorphism.

The mass-continuity equation requires that any change of mass density ρ in time t must be compensated by a divergence in the flux of mass:

$$\partial\rho/\partial t + \nabla(\rho v) = 0, \tag{1}$$

where v is velocity. Two approximations are commonly applied to this equation. The first is the well-known Boussinesq approximation (Boussinesq 1897), which assumes that density differences are sufficiently small to be neglected, except in the buoyancy term. Therefore density – and hence volume – changes due to deformation are neglected (Figs 1a and b), and eq. (1) is simplified to the incompressible flow formulation:

$$\nabla v = 0. \tag{2}$$

This approximation is made in the overwhelming majority of numerical geodynamic models (e.g. Burov *et al*. 2001 based on Poliakov *et al*. 1993; Kaus *et al*. 2005; Arcay *et al*. 2007; Yamato *et al*. 2007; Braun *et al*. 2008; Rey & Müller 2010). The second approximation concerns the implementation of metamorphism. In simpler cases the inherent variations in density due to varying pressure–temperature (P–T) conditions are not taken into account (Fig. 1a). In more complex models, density changes as a function of P and T, but the induced deformation (volume change) is neglected (Fig. 1b). Physically, the first term $\partial\rho/\partial t$ of eq. (1) is respected, but the second term $\nabla(\rho v) = v{\cdot}\nabla\rho + \rho{\cdot}\nabla v$ is simplified to eq. (2) by neglecting the density change driven volumetric variation $v{\cdot}\nabla\rho$.

There are – to our knowledge – only three modelling tools using the complete form of mass-continuity (Gerya & Yuen 2007; Warren *et al*. 2008 and subsequent works; Afonso & Zlotnik 2011), but differences with respect to previous (incompressible) models are not discussed.

In this paper we advocate for a complete (compressible) solution of the continuity equation that includes the full flow field induced by density changes (Fig. 1c). We argue that the oft-used Boussinesq approximation and metamorphic density changes (exceeding 15 per cent, e.g. Holmes 1965; Liu 1978) have significant

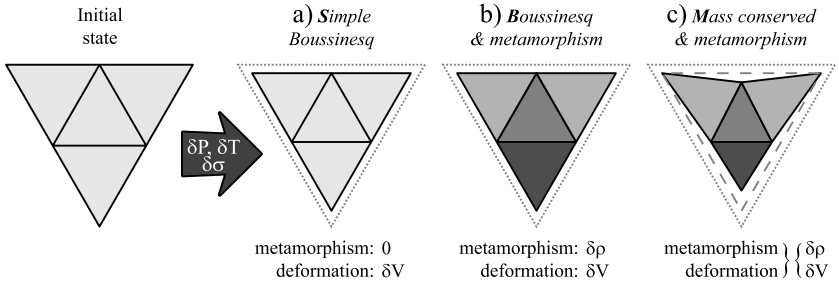

Figure 1. Implementations of metamorphism and deformation into numerical models. Schematic finite elements show changes from the initial state through deformation and varying pressure-temperature conditions (arrow). (a) The simplest models do not account for metamorphism and do not include density variations, even when deformation affects the volume (S model). (b) In the Boussinesq formulation including metamorphism, densities vary as prescribed by phase equilibria calculations, but volume changes are still driven by deformation (B model). Both of the above implementations violate mass-continuity in that volume and density vary independently. (c) Volumetric changes are enforced following density changes according to mass-continuity (M model).

consequences for geodynamic models. Using a simple example, we provide the first direct and quantitative assessment of the continuity-equation formulation's volumetric effects on lithospheric deformation pattern. We focus on this example to draw attention to the potential problems caused by the Boussinesq approximation.

2 METHODS

We focus on the physical effect of the continuity equation formulation and metamorphism by consistently adjusting volume related to mass-continuity when density changes are present (Fig. 1c). Subsequently, we compare the results with those from approximated formulations to assess the consequences on the deformation field.

To account for metamorphic density changes in the *P–T* space we introduce a 'metamorphic' strain tensor that modifies the total strain field of the entire modelled geodynamic system (i.e. applies to all deforming elements, not only those undergoing phase change).

$$\varepsilon^{\text{sys}} = \varepsilon^{\text{sys}} - \varepsilon^{\text{metam}}. \tag{3}$$

Assuming isotropic deformation the metamorphic strain is derived directly from the required density change to respect mass conservation at the element scale:

$$\varepsilon_{ii}^{\text{metam}} = 1/3 \cdot \Delta v/v = -1/3 \cdot \Delta\rho/\rho \ (i = 1, 3), \tag{4}$$

where $\Delta\rho$ is the density change prescribed by phase equilibria calculations. This approach is implemented into a thermo-mechanical finite element modelling tool Cast3M (Verpeaux *et al*. 1988; http://www-cast3m.cea.fr/). This tool features a 2-D geodynamic toolbox that simulates different rheological behaviours, erosion processes and re-meshing. For full details, including resolution scheme, numerical tests, comparisons with other geodynamic modelling tools as well as applications, we refer to Godard *et al*. (2006, 2009) and references therein. An alternative method of accounting for metamorphic density changes would be to express the equation of state as a function of entropy and volume (Connolly 2009). The virtue of this method is that it eliminates singularities in the *P–T* space related to low-order phase transformations. The method is not investigated here because it requires a non-standard numerical formulation, the implementation of which is beyond the scope of this paper.

Our implementation of metamorphic effects follows eqs (3) and (4) with two adaptations for Cast3M: (1) the metamorphic strain is converted to an elastic metamorphic stress because in our implementation stress is the global variable governing the system's deformation; (2) the metamorphic stress is damped to avoid large perturbations in the system – the element's density (volume) will not reach the prescribed value instantaneously, but over a few or few tens of time steps. Because the numerical model involves a large number ($\sim 10^5$–10^6) of time steps we expect and verify that this convergence takes place. Our approach using eq. (3) is straightforward, and does not require major modifications in the numerical resolution scheme of the code. Further details on the implementation are given in Appendix S1 (see Supporting Information).

The three modelling studies mentioned previously that solved the complete form of mass-continuity all used different implementations. Gerya & Yuen (2007) apply a plastic flow rule to express and introduce volumetric changes in terms of dilatant plastic deformation rate. Warren *et al*. (2008) first solve the incompressible formulation (eq. 2) and then add a correcting term in the form of normal forces changing the size of elements, but only during time steps when phase changes take place (therefore this approach does not enforce mass conservation of deforming regions remaining in the same phase). Afonso & Zlotnik (2011) also assume an incompressible media, and apply a local velocity field in the lithosphere that compresses/expands the material undergoing phase change. None of the three models discusses the effect of introducing volumetric changes in their models; therefore a comparison to our procedure and results is infeasible.

3 MODEL SETUP

Our setup simulates intracontinental mountain building following the approach of Avouac & Burov (1996), with, in addition, lower crustal eclogitization. The temporal evolution of a 2-D viscoelastic lithospheric model composed of three layers is analysed, starting with an initial topography and crustal root (Fig. 2). The model imposes horizontal convergence, and accounts for gravitational forces, basal heat flow from the underlying mantle and radiogenic heat production in the crust. The initial temperature field is calculated in steady state at the first time step and is shown in Fig. 2. We simulate surface processes as linear diffusion (e.g. Avouac & Burov 1996), which is a voluntarily simplified but a mass-conserving scheme. Description and quantification of these parameters are shown in Fig. 2 and detailed in Appendix S1.

Metamorphic density changes are anticipated to be the greatest in the lower crust (eclogitization); therefore, for the sake of simplicity and numerical efficiency, we assume constant density for the other layers. In the lower crust, the petrogenetic *P–T–ρ* grid is precalculated using Perple_X (Connolly 2005) using an average lower crustal composition and the procedure proposed in Heténi *et al*. (2007) (see Fig. A2 in Appendix S1). We implement the three formulations of the continuity-equation detailed earlier (Figs 1a–c), and

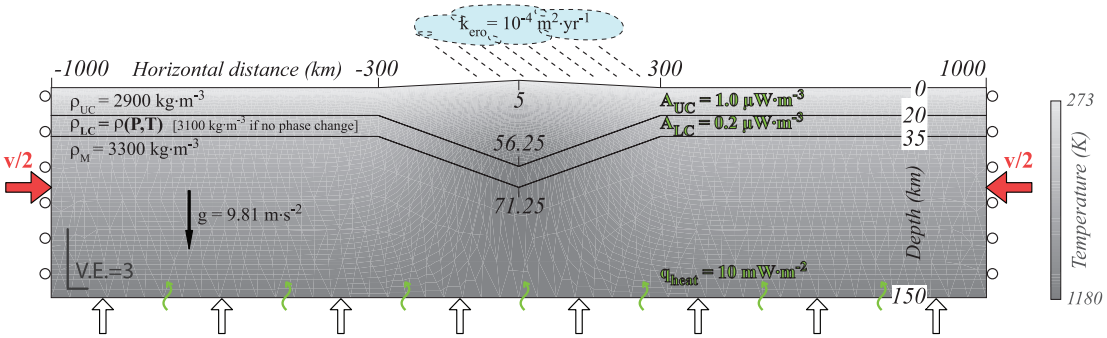

Figure 2. General setup, geometry and the initial temperature field of the model. Modelled geodynamic processes include erosion at surface and metamorphism in the lower crust. These processes as well as boundary conditions are described in the text and in Appendix S1, the resolution of the model is shown in Fig. A1 in Appendix S1.

compare the deformation pattern after a time period of ∼3 Myr. This comparison starts after an initial time of 0.6 Myr during which the main processes (convergence, erosion and metamorphism) are introduced gradually to avoid perturbations at start-up (Appendix S1).

4 RESULTS

We characterize the deformation pattern by focusing on the shape of the topography and of the densifying crustal root. Their evolution in time is visualized through a few characteristic parameters representative of their shape (Fig. 3a). We compare the evolution of these parameters over ∼3 Myr after the initiation time (Figs 3b–g) in the three main models:

(1) the S model with the Boussinesq approximation and without metamorphism (Fig. 1a);
(2) the B model with the Boussinesq approximation and with independent metamorphism (Fig. 1b), which is currently the most widely used type of geodynamic model;
(3) the M model with mass-conservation and with linked metamorphism (Fig. 1c).

The comparison of the deformation patterns' evolution with our simulation settings can be summarized as follows (Figs 3b–g, see density profiles on Fig. A3).

The formulation of metamorphism has no apparent effect on the width of the topography at its base. However, all three models are wider than the initial geometry due to the lateral distribution of material dictated by the diffusive erosion formulation we use.

The mass-conserving formulation creates a similar but slightly (∼3 per cent in 3.2 Myr) higher relief compared with the simple model. Accounting for density variations in the Boussinesq approximated model produces a significantly (∼25 per cent) lower relief and misleadingly suggests greater negative buoyancy associated with metamorphism. This is due to the artificially increased mass of the lower crust as it undergoes eclogitization (higher density, but no decrease of volume). The increasing trend with time is due to continuing horizontal convergence.

The evolution of the foreland basin depth shows large differences: while adding density variations to the S model causes a shallower (∼19 per cent in 3.2 Myr) basin (B model), correcting for the volumetric effects results in a significantly (approximately a factor of 2) deeper basin (M model). The latter effect is related to the more localized downward traction of the densifying crustal root that enhances lateral advection of material from the shoulder area towards the centre of the model. The deeper foreland basin largely contributes to the higher relief (Fig. 3b). In the B model the neglect of the volumetric changes hampers deformation localization and the overall deformation pattern is laterally more distributed.

The base width of the crustal root appears to be controlled by the volumetric effect. When this is correctly implemented, the active orogen has a narrower underlying root due to the increasing density and decreasing volume. The M model's narrowing is greater by 67 per cent relative to the S and B models (with our model settings, at 3.2 Myr). In the incompressible cases (S and B model), in which volume changes are neglected, localization is not enhanced, and this is irrespective of density changes. The general decreasing trend with time is due to the continuing horizontal convergence.

The maximum deepening of the Moho root compared to its initial position shows a faster trend in the case where mass conservation is respected. The B model initially exaggerates the deepening of mass-continuity respecting model due to the artificially increased mass of the crustal root.

The average slope of the crustal root derives from the two previous pictures: a steeper deepening when both mass-continuity and metamorphic density changes are respected. The B model's slope (accidentally) falls near the complete solution by its wider base-width and exaggerated deepening.

Our results suggest that – in addition to convergence, the assumed rheology and surface processes – the implementation of the continuity equation also has important consequences for the evolution and localization of deformation. The principal physical development of the model we propose compared to the previous generations is that it includes both density and strictly bound volume changes that shape the geometry at depth and at surface. In our setup, the density change drives a faster deepening of the lower crustal root relative to models without metamorphism; the volume change avoids the artificial mass generation of the Boussinesq approximation and creates a horizontally narrower, more localized root. Both effects combined make that the horizontal convergence is more efficiently accommodated and converted into vertical mass movement in the orogen, into the deeper root and the higher relief. Hence metamorphic phase changes in combination with the more rigorous implementation of continuity produce a distinctly different deformation pattern and evolution trend than obtained with the various approximations.

To demonstrate the robustness of our approach, the evolution of the total mass of the system with time shows how accurately mass conservation is respected (Fig. 4). While the models lacking a proper implementation of mass-continuity are in constantly increasing error, the model with a consistent implementation continuously respects mass conservation (its deviation from the initial mass is less than the mass of the smallest element, and can be related to numerical noise). At the end of the simulation the total mass in the

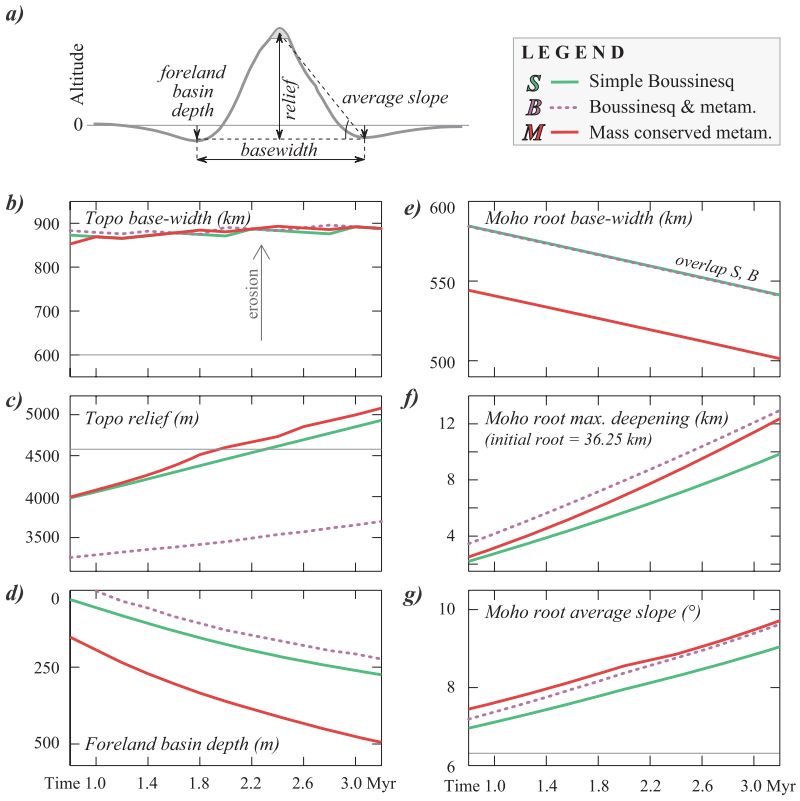

Figure 3. (a) Definition of the parameters describing the shape of the topography high (or, inversely, of the Moho root). The mean altitude of the peak is averaged over 100 km horizontal distance. (b)–(g) Deformation of the model in the three different setups: evolution of the shape parameters describing the geometry of the topography (b–d) and Moho root (e–g). Horizontal thin lines (b, c and g) correspond to the initial level of the values. See text for discussion.

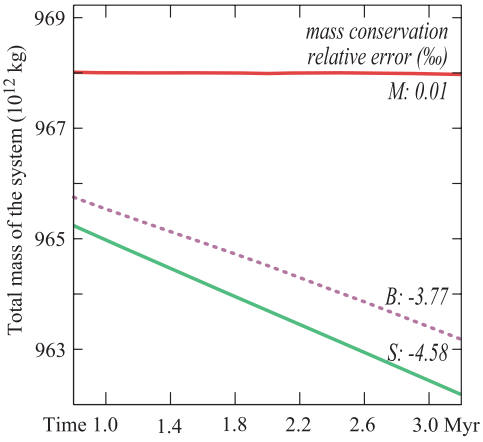

Figure 4. Total mass of the system and the evolution of error for the three models. Relative error is shown at 3.2 Myr. Time is the effective simulation time after the initiation time.

M model records a relative change of 10^{-5}. This is about 2.5 orders of magnitude more accurate than in models with approximated effects of deformation and metamorphism.

5 IMPLICATIONS AND CONCLUSIONS

We showed that the correct implementation of the mass-continuity equation has potentially important consequences on models of lithospheric deformation including metamorphism. To illustrate the effects on the deformation pattern, we built a simple orogenic model, which demonstrates that metamorphism has a key role in shaping the lithospheric structure. Our model also illustrates that the widely used incompressible formulation (Boussinesq approximation) may introduce inaccuracies in mass-continuity and exhibit misleading trends in deformation, in particular when used in conjunction with metamorphic phase changes.

The implications of modelling metamorphism in a physically correct manner are manifold. For instance:

(1) Numerical simulations aiming to reproduce the evolution of exhumation, surface uplift or foreland basin development may be in error when using approximated formulations of mass-continuity. The error is model dependent, but may exceed a factor of 2 for some model parameters as demonstrated by our results on the foreland basin depth. Errors of this magnitude are such that a revision of the previously inferred rates may be necessary to match the same data.

(2) Geologically fast density (and corresponding volume) changes are likely to generate stresses large enough to create fractures or trigger fracturing at depth. The induced stresses can easily exceed the order of a few bars, which is comparable to the stress-drop deduced for earthquakes (Hanks 1977; Scholz 1990). A currently active field example can be the eclogitization of the Indian lower crust beneath Tibet, which spatially coincides with a zone of microseismic activity (Hetényi *et al*. 2007; Whittlinger *et al*. 2009). The accurate resolution of these stresses in geodynamic models requires rigorous solution of the continuity equation.

(3) Metamorphism is shown to influence the shape of the crustal root. In studies where the flexural geometry of a plate is used to estimate lithospheric rheology (e.g. Cattin *et al*. 2001; Hetényi *et al*. 2006; and references therein), a revision of the numerical model may modify the assessed mantle viscosities and lithospheric effective

elastic thickness. The volumetric effects similarly determine the mass distribution and the pressure field within the crustal root and have implications for HP-UHP exhumation processes (e.g. Yamato *et al*. 2007).

(4) If densification and the downward drag of the crustal root are accompanied with rheological softening, the root may become unstable during the long-term evolution of the orogen and enhance decoupling or break-off. The timing of such event will depend on the weight of the crustal root. Incorrect mass estimates resulting from the Boussinesq approximation are likely to lead to false assessment of the timing of decoupling or break-off scenarios and lead to biased conclusions.

Correct modelling of metamorphism that complies with mass conservation is therefore essential to understand long-term tectonic evolution and to assess the respective importance of the different geodynamic processes involved.

ACKNOWLEDGMENTS

We acknowledge the numerous people from ENS Paris and ETH Zurich who provided us with feedback on metamorphism and its effects on geodynamics. In particular we thank Paul Tackley and Taras Gerya for discussion on continuity equation literature, and Alan B. Thompson for his recurrent support and considered opinion. Feedback from attendees at the EGU 2010 conference helped to finalize an earlier draft of the manuscript, which also benefited from the constructive review of J. C. Afonso. We finally thank Philippe Yamato and an anonymous person for their rapid and constructive reviews. This work was supported by the Swiss National Science Foundation grant 200020-107889.

REFERENCES

Afonso, J. C. & Zlotnik, S., 2011. The subductability of the continental lithosphere: the before and after story, in *Frontiers in Earth Sciences, Arc-Continent Collision,* Springer, Berlin, in press.

Arcay, D. *et al.*, 2007. Influence of the precollisional stage on subduction dynamics and the buried crust thermal state: insight from numerical simulations, *Tectonophysics,* **441**, 27–45, doi:10.1016/j.tecto.2007.06.001.

Avouac, J.-P. & Burov, E., 1996. Erosion as a driving mechanism of intracontinental growth, *J. geophys. Res.,* **101**, 17 747–17 769, doi:10.1029/96JB01344.

Boussinesq, M. J., 1897. *Théorie de l'écoulement tourbillonnant et tumultueux des liquides dans les lits rectilignes a grande section,* pp. 1–64, Gauthier-Villars et fils, Paris.

Braun, J. *et al.*, 2008. DOUAR: a new three-dimensional creeping flow numerical model for the solution of geological problems, *Phys. Earth planet. Inter.,* **171**, 76–91, doi:10.1016/j.pepi.2008.05.003.

Burov, E. *et al.*, 2001. A thermomechanical model of exhumation of high pressure (HP) and ultra-high pressure (UHP) metamorphic rocks in Alpine-type collision belts, *Tectonophysics,* **342**, 113–136.

Cattin, R. *et al.*, 2001. Gravity anomalies, crustal structure and thermomechanical support of the Himalaya of Central Nepal, *Geophys. J. Int.,* **147**, 381–392.

Connolly, J. A. D., 2005. Computation of phase equilibria by linear programming: a tool for geodynamic modeling and its application to subduction zone decarbonation, *Earth planet. Sci. Lett.,* **236**, 524–541.

Connolly, J. A.D., 2009. The geodynamic equation of state: what and how, *Geochem. Geophys. Geosyst.,* **10**, Q10014, doi:10.1029/2009GC002540.

Cserepes, L. *et al.*, 1988. Three-dimensional infinite Prandtl number convection in one and two layers with implications for the Earth's gravity field, *J. geophys. Res.,* **93**, 12 009–12 025.

Gerya, T.V. & Yuen, D.A., 2007. Robust characteristics method for modelling multiphase visco-elasto-plastic thermo-mechanical problems, *Phys. Earth planet. Inter.,* **163**, 83–105.

Godard, V. *et al.*, 2006. Numerical modelling of erosion processes in the Himalayas of Nepal: effects of spatial variations of rock strength and precipitation, *Geol. Soc. London Spec. Pub.,* **253**, 341–358.

Godard, V. *et al.*, 2009. Erosional control on the dynamics of low-convergence rate continental plateau margins, *Geophys. J. Int,* **179**, 763–777, doi:10.1111/j.1365-246X.2009.04324.x.

Hanks, T., 1977. Earthquake stress-drops, ambient tectonic stresses, and stresses that drive plates, *Pure appl. Geophys.,* **115**, 441–458.

Hetényi, G. *et al.*, 2006. The effective elastic thickness of the India Plate from receiver function imaging, gravity anomalies and thermomechanical modeling, *Geophys. J. Int.,* **167,** 1106–1118, doi:10.1111/j.1365-246X.2006.03198.x.

Hetényi, G. *et al.*, 2007. Density distribution of the India plate beneath the Tibetan Plateau: geophysical and petrological constraints on the kinetics of lower-crustal eclogitization, *Earth planet. Sci. Lett.,* **264**, 226–244.

Holmes, A., 1965. *Principles of Physical Geology,* 2nd edn, pp. 1–1288, Thomas Nelson and Sons Ltd., London.

Kaus, J.P.B. *et al.*, 2005. Effect of mineral phase transitions on sedimentary basin subsidence and uplift, *Earth planet. Sci. Lett.,* **233**, 213–228.

Liu, L.-G., 1978. High-pressure phase transformations of albite, jadeite and nepheline, *Earth planet. Sci. Lett.,* **37**, 438–444.

Poliakov, A.N.B. *et al.*, 1993. Initiation of salt diapirs with frictional overburden: numerical experiments, *Tectonophysics,* **228**, 199–210.

Rey, P. F. & Müller, R. D., 2010. Fragmentation of active continental plate margins owing to the buoyancy of the mantle wedge, *Nature Geosci.,* **3**, 257–261, doi:10.1038/ngeo825.

Scholz, C., 1990. *The Mechanics of Earthquakes and Faulting,* pp. 1–439, Cambridge University Press, Cambridge.

Verpeaux, P. *et al.*, 1988. Castem2000: une approche moderne du calcul des structures, in *Calcul des Structures et Intelligence Artificielle,* pp. 261–271, eds Fouet, J. M. *et al*., Pluralis, Paris.

Warren, C. J. *et al.*, 2008. Formation and exhumation of ultra-high-pressure rocks during continental collision: role of detachment in the subduction channel, *Geochem. Geophys. Geosyst.,* **9**, Q04019, doi:10.1029/2007GC001839.

Whittlinger, G. *et al.*, 2009. Seismic velocities in Southern Tibet lower crust. A receiver function approach for eclogite detection, *Geophys. J. Int.*, **177**, 1037–1049.

Yamato, P. *et al.*, 2007. Burial and exhumation in a subduction wedge: mutual constraints from thermomechanical modeling and natural P-T-t data (Schistes Lustrés, western Alps), *J. geophys. Res.,* **112**, B07410, doi:10.1029/2006JB004441.

SUPPORTING INFORMATION

Additional Supporting Information may be found in the online version of this article:

Appendix S1. This appendix includes details on: the model setup and input parameters (Section A1); time and timing of processes (A2); the implementation of metamorphism (A3) and numerical limitations (A4) including the corresponding figures.

Please note: Wiley-Blackwell are not responsible for the content or functionality of any supporting materials supplied by the authors. Any queries (other than missing material) should be directed to the corresponding author for the article.